ELSEVIER

Thermochimica Acta 329 (1999) 97–108

thermochimica acta

Systematic calorimetric study of glass transition in the homologous series of poly(*n*-alkyl methacrylate)s: Narayanaswamy parameters in the crossover region

E. Hempel, S. Kahle, R. Unger, E. Donth*

Universität Halle, Fachbereich Physik, D-06099 Halle, Germany

Received 17 August 1998; accepted 20 December 1998

Abstract

The glass transition in poly(*n*-alkyl methacrylate)s from C=1 (methyl, PMMA) over 2, 3, 4, 5, 6, 7, to C=9 (nonyl) is investigated by differential scanning calorimetry DSC, and partly by temperature modulated DSC, TMDSC. The results are compared with dielectric and heat capacity spectroscopy so far as available. The DSC thermograms are evaluated by a modified Narayanaswamy model MNM that permits a point-by-point determination of the underlying equilibrium trace of the dynamic glass transition in an Arrhenius diagram. The MNM parameters and their variations due to differently given Vogel temperatures are discussed and compared with literature values for polyvinylacetate PVAC and polystyrene PS. It seems not possible at present to determine a definite Narayanaswamy mixing parameter x for a substance as such, e.g. for PVAC and PS, the uncertainty is about $\Delta x = \pm 0.2$. For the homologous P*n*AMA series dramatic changes of x outside the Δx uncertainty are observed near the crossover region. The results are discussed with respect to cooperativity, fragility, vitrification rate, and further characteristics of the glass transition.

Keywords: Poly(*n*-alkyl methacrylates); Calorimetry; Glass transition; Vitrification; Narayanaswamy parameters

1. Introduction

Several poly(*n*-alkyl methacrylates)s P*n*AMAs were investigated by differential scanning calorimetry DSC [1–4], temperature modulated DSC, TMDSC [5], and heat capacity spectroscopy HCS [6,7] in the glass transition region. As obtained by dielectric spectroscopy [8–10], the Arrhenius diagram ($\log \omega$ versus $1/T$) displays the typical crossover scenario (Fig. 1) with three processes: the high-temperature a process (''cage escape'' [11]), the low-temperature α process (''cooperative''), and the Johari Goldstein β process (''local'' relaxation [8,12,13]). The main calorimetric effects come from the α and a processes since the local β relaxation has usually a very low calorimetric activity [14].

The enlargement of the C number of the *n*-alkyl side group along the homologous series of P*n*AMAs shifts the ''splitting region'' of Fig. 1 to lower frequency, approximately one frequency decade per C atom. Since the β trace is nearly fixed in the Arrhenius diagram the glass temperature is lowered correspondingly. The crossover arrives at the ''glass frequency'' or ''freezing frequency'' which corresponds to a cooling/heating rate $\dot{T} = 10\,\mathrm{K/min}$ for about C=6 (hexyl)

*Corresponding author. Fax: +49-345-55-27017; e-mail: donth@physik.uni-halle.de

0040-6031/99/$ – see front matter
PII: S0040-6031(99)00011-8

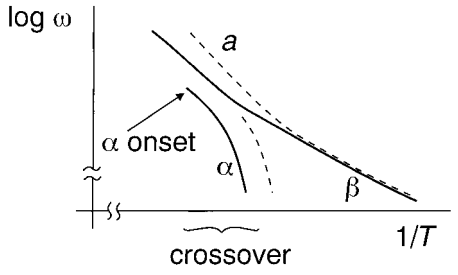

Fig. 1. Schematic dielectric splitting scenario of the crossover region of two P*n*AMAs of different C numbers for the alkyl side chain. Larger C numbers shift the a and α processes to lower temperatures T and frequencies ω.

or C=7 (heptyl) in the P*n*AMA series of conventional tacticity. This means that DSC measures the α process for C≤5 (pentyl) and the a process for C≥8 (octyl). The crossover region of P*n*AMAs can thus be scanned by systematic variation of the *n*-alkyl C number.

Vitrification can be modeled by the Narayanaswamy model [15]. This model is usually characterized by four or five parameters:

$$\{x, \beta, B, \tau_b; T_\infty\}. \tag{1}$$

The Narayanaswamy mixing parameter x, $0 \le x \le 1$, defines the weight of the actual temperature: for $x=0$ the vitrification is determined by the fictive temperature T_f [16], for $x=1$ by the actual temperature T. The β parameter defines the non-exponentiality of the underlying equilibrium relaxation function, e.g. by a Kohlrausch Williams Watts stretched exponential: $\beta = \beta_{KWW}$ [17,18]. B is the (effective) slope of the α or a trace in the Arrhenius diagram at T_g,

$$B = -\mathrm{d}\ln\tau/\mathrm{d}T|_{T_g}. \tag{2}$$

This is a measure of the calorimetric fragility. The corresponding steepness index [19] is

$$m_c = -\mathrm{d}\log\tau/\mathrm{d}\ln T|_{T_g} = T_g \cdot B/\ln 10. \tag{3}$$

The reference time τ_b depends on an arbitrary reference temperature T_b, $\log \tau_b$ (T_b). High-precision modeling needs also a curvature of the α or a trace in the Arrhenius diagram: we take a local WLF [20] equation for $\log\tau(T)$ or $\log\omega(T)$, the curvature increases with the Vogel temperature T_∞ used ($T_\infty=0$ means no curvature).

We are interested in the following question: is the change from the α process to the a process in the crossover region calorimetrically indicated by DSC, especially by the behavior of the mixing parameter x? To qualify this question we apply two concepts:

1. *Informative zone*. The parameters x, β, and B should be stable against moderate variations of T_b and T_∞. On the other hand, these parameters can reasonably be determined only from that temperature region of the $C_p(T)$ step where x, β, and B really affect the $C_p(T)$ model. This zone is scanned by using a modified Narayanaswamy model (MNM) as described in Section 2 below: the parameters x, β, and B where determined as a function of a systematic T_b scan. The informative zone is defined as the T_b temperature region where the $\log\tau_b(T_b^{-1})$ trace reproduction in the Arrhenius diagram is not too sensitive to T_b or moderate T_∞ variations. A further test is a certain stability of the parameters in this zone. The lower boundary of the informative zone is fixed at T_g (Fig. 2) to prevent unrealistic extrapolations for low frequencies.
2. α *Cooperativity onset*. We observed by means of systematic HCS investigations [21–23] below the α onset (Fig. 1) that

$$N_\alpha^{1/2} \sim (T_{on} - T),\ T < T_{on}, \tag{4}$$

where

$$N_\alpha \equiv RT^2\Delta(1/C_V)/(M_0\delta T^2) \approx RT^2\Delta C_p/(M_0\bar{C}_p^2\delta T^2) \tag{5}$$

N_α is a measure of the α cooperativity. It is determined by Eq. (5), i.e. a formula from thermodynamic fluctuation theory [24–26]. All variables on the right-hand side of Eq. (5) can be determined from calorimetry: ΔC_p is the $C_p(T)$ step at the glass transition, $\bar{C}_p = (C_p^g + C_p^l)/2$ the average of glass and liquid zone specific heat capacity, and δT the width (dispersion) of the $C_p''(T)$ peak at given

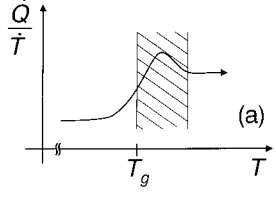

Fig. 2. Informative zone of a DSC thermogram. Details see text.

frequency. We use [25]

$$\delta T = 1/B\beta. \tag{6}$$

M_0 is the molecular mass of what is considered a particle (the monomeric unit here), and R the universal gas constant.

Usually, N_α is of order 100 at the glass temperature in case it is far below the crossover. But HCS on the hexyl member (P*n*HMA, C=6) showed that the a process has also a small N_α of order 1 decreasing slightly with increasing temperature.

The aim of this paper is a systematic DSC and TMDSC study in the homologous P*n*AMA series to determine the informative zone of glass transition and to determine the behavior of calorimetric parameters in the crossover region of P*n*AMAs, especially the cooperativity N_α and the Narayanaswamy mixing parameter x.

2. Modified Narayanaswamy model MNM

The Narayanaswamy model is modified by the possibility to adjust the parameter set of Eq. (1) for any given T_∞ and T_b value. The determination of the parameters of an underlying complete WLF curve

$$\ln \tau_b(T_b) = -\ln \Omega + B(T_g - T_\infty)^2/(T_b - T_\infty), \quad \Omega = 1/\tau_0, \tag{7}$$

from DSC scans is well known [1,27]. Our modification allows a point by point determination of the underlying equilibrium trace $\log \tau_b(T_b^{-1})$ in the informative zone of the Arrhenius diagram, irrespective of their local modeling by WLF. The power of the modification was demonstrated for the hexyl member, P*n*HMA. Some features of the crossover peculiarity for P*n*HMA as determined by HCS [7] could be reproduced by the MNM equilibrium trace from DSC [28].

In formulas, Tool's fictive temperature [16], T_f, is defined by

$$T_f(t) = T(t) - \int_{t_0}^{t} \mathrm{d}T' \phi(\Delta\zeta), \quad T' = T(t'), \tag{8}$$

where the integral is over the history $T(t')$, starting at a time t_0 with $T(t_0)$ in equilibrium. The response function is chosen, according to Moynihan et al. [17], as a Kohlrausch function,

$$\phi = \exp[-(\Delta\zeta)^\beta], \quad 0 < \beta \le 1, \tag{9}$$

with a Kohlrausch exponent $\beta(=\beta_{KWW})$. The dimensionless material time difference between t and t' is defined by

$$\Delta\zeta = \zeta(t) - \zeta(t') = \int_{t'}^{t} \mathrm{d}t'/\tau_s,$$

where τ_s counts the time (τ_0) of the material clock. This time is influenced by both the actual (T) and fictive (T_f) temperature weighted by the Narayanaswamy mixing parameter x [15],

$$\tau_s = \tau_0 \exp\left[B(T_g - T_b)^2\left(\frac{x}{T - T_\infty} + \frac{1-x}{T_f - T_\infty}\right)\right], \quad 0 < x < 1. \tag{10}$$

The equilibrium reference time $\tau_b(T_b)$ is defined by

$$\tau_b = \tau_0 \exp[B(T_g - T_\infty)^2/(T_b - T_\infty)]. \tag{11}$$

The relation to an apparent activation enthalpy $\Delta h'$ often used in the literature [29] is

$$B \equiv -\mathrm{d}\ln\tau/\mathrm{d}T|_{T_g} = \Delta h'/T_g^2 R. \tag{12}$$

The calculation consists of iterations, where, as usual, the time history is broken into a sequence of n suitably chosen time intervals k:

$$T_f^{(n)} = T^{(n)} - \sum_{k=1}^{n} (\Delta T/\Delta t)^{(k)} \phi^{(k)} \Delta t^{(k)}, \quad k = 1, 2, \ldots, n, \tag{13}$$

with

$$\phi^{(k)} = \exp\left\{ -\left(\frac{1}{\tau_b}\sum_{i=k}^{n} \exp\left[B(T_g - T_\infty)^2\left(\frac{1}{T_b - T_\infty} - \left(\frac{x}{T^{(i)} - T_\infty} + \frac{1-x}{T_f^{(i-1)} - T_\infty}\right)\right)\right]\Delta t^{(i)}\right)^\beta\right\}, \tag{14}$$

and i=k, k+1, …, n. The relation between the DSC curve ($C_p(T)$) and the fictive temperature,

$$\frac{\mathrm{d}T_f}{\mathrm{d}T}(T) = \frac{C_p(T) - C_{p,g}(T)}{C_{p,l}(T) - C_{p,g}(T)}, \tag{15}$$

is sensitive to the construction of liquid and glass tangents at the C_p curve, $C_{p,l}(T)$ and $C_{p,g}(T)$, respectively. This is a serious problem for the higher poly(*n*-alkyl methacrylate)s (C>9) because a second polyethylene-like glass transition intervenes [30–32].

After the input of $\{T_\infty, T_b, T_g\}$, where T_g is from an equal-area construction, and of a given temperature–time program, $(\Delta T/\Delta t)^{(k)}$, we get, from an adjustment of the iteration loops Eqs. (13) and (14), the parameter set

$$\{x, \beta, B, \tau_b\} \tag{16}$$

for any given T_b and T_∞. Formally, inserting τ_b from Eq. (11) into Eq. (14), both τ_b and T_b are cancelled, and Eqs. (13)–(15) do not seem to contain any information on $\tau_b(T_b)$. But, giving only T_b as an input and determining τ_b separately from a fit we get an actual value for τ_b for each T_b! If we repeat the adjustments for different T_b input values we obtain, point by point, different τ_b values: $\tau_b=\tau_b(T_b)$ is the desired underlying equilibrium function of reference times. As mentioned above, our local method is different from a subsequent calculation of $\tau_b(T_b)$ according to Eq. (11) after a global fit of its parameters [1].

Practically we start with initial values $\{x_{start}, \beta_{start}, B_{start}\}$ and with a set of $T_{b\,start}^{(l)}$ temperature values, e.g. $T_{b\,start}^{(l)} = T_g - 10\,K,\ T_g - 5\,K,\ \ldots,\ T_g + 20\,K,\ l = 1, 2, \ldots, N$. The latter correspond to an N set of $\tau_{b\ start}$ values (e.g. from one WLF curve of dielectric measurements).

We use the two alternative iterations:

(i) *Average continuation*. The first adjustment run results in new average values

$$x_{new} = N^{-1}\sum_{l=1}^{N} x_l, \qquad \beta_{new} = N^{-1}\sum_{l=1}^{N} \beta_l,$$

$$B_{new} = N^{-1}\sum_{l=1}^{N} B_l \tag{17}$$

and a new set of $\tau_{b\,new}^{(l)}(T_b)$ values. These new values from the preceding run are used as start values of the next run, and so on until the new values become stable. The final result corresponds to a fix point of the iteration and is denoted by

$$\{\bar{x},\ \bar{\beta},\ \overline{B},\ \tau_b^{(l)}(T_b^{(l)})\}. \tag{18}$$

This iteration is fast and well-suited when no peculiarities in the equilibrium $\log \tau_b(T_b^{-1})$ trace are expected (as e.g. far above or far below the crossover=splitting region).

Table 1
Comparison of MNM parameters of P*n*BMA for the two iteration variants for $T_\infty=T_g-50$ K$=-25$°C

	(i)	(ii)
B (K^{-1})	0.635±0.014	0.651±0.010
x	0.311±0.006	0.303±0.005
β	0.310±0.003	0.307±0.002
$\delta T/K$	5.08±0.07	5.00±0.05

(i) Average continuation, (ii) fixed start values. The parameters are mean values in the informative zone (from $T_b=T_g=25$°C to $T_b=47$°C).

(ii) *Fixed start values* of x, β, and B are used for all iterations. Only the new $\tau_b^{(l)}(T_b)$ values of the preceding iteration are used for the next iteration. This method is slower, but should be used when peculiarities in the $\log \tau_b(T_b^{-1})$ trace are expected, i.e. if the crossover is in the informative zone. In P*n*HMA, for instance, the start times $\log \tau_b$ should be longer than the stable relaxation times of the a relaxation, because then the first-coming a trace is only a secondary optimization minimum. The absolute minimum is the virtual WLF continuation of the α trace beyond the $a\beta$ trace [28].

The parameter differences between the two variants are usually small (Table 1).

After the iterations, the final values are tested against their stability with respect to a T_∞ variation. We choose different T_∞ values, e.g. T_g-50 K, T_g-60 K, ..., and $T_\infty=0$ K (Arrhenius), and repeat the adjustment iterations.

2.1. Important remark

In this work, we apply the MNM only to the heating phase of a linear, symmetric $T(t)$ cooling–heating cycle between temperatures far above and far below T_g, with only a few minutes equilibration at the lowest temperature. If the Narayanaswamy model is exact the parameters obtained from different $T(t)$ programs would be the same. This is not the case. In some examples we observed considerable variations of the Narayanaswamy parameters for different annealing times and temperatures in the transformation interval. This means that our parameters should really be

labeled by the $T(t)$ program used. General limits of the Narayanaswamy model are discussed in [33].

3. Experimental

The poly(ethyl methacrylate) (PEMA) and poly(*n*-butyl methacrylate) P*n*BMA samples were purchased from Polyscience, poly(*n*-nonyl methacrylate) (P*n*NMA) was purchased from Polymer Sources. Poly(*n*-propyl methacrylate) P*n*PrMA, poly(*n*-pentyl methacrylate) P*n*PenMA, poly(*n*-heptyl methacrylate) (P*n*HepMA), and poly(*n*-lauryl methacrylate) (P*n*LMA) were kindly polymerized by Dr. S. Zeeb (Halle). Poly(*n*-hexyl methacrylate) (P*n*HMA) was kindly provided by Dr. G. Meier (Jülich). Poly(methyl methacrylate) (PMMA) is a commercial product. All samples were synthesized by radical polymerization, except the sample P*n*NMA which was anionically polymerized. The molecular masses of the samples range from 72 to 330 kg/mol. As typical for radical polymerization, $\overline{M_w}/\overline{M_n}$ ranges from 1.9 to 2.45, $\overline{M_w}/\overline{M_n}$ for P*n*HMA is 1.26, and the (diade) syndiotacticity is between 68% and 79%. Polystyrol PS 168 N from BASF (M_n=270 kg/mol) and PVAC (M_n=407 kg/mol) are commercial products.

All samples were dried under vacuum for 12 h at a temperature of about T=+80°C. The sample weights were about 10 mg.

A DSC 7 apparatus (Perkin-Elmer) was used for a cooling–heating cycle between about T_g+50 K and T_g−100 K with rates of $|dT/dt|$=10 K/min. The annealing time between cooling and heating was 5 min. The glass temperature T_g was calculated by an equal-area construction using the two tangents, far below and far above the transformation interval [29]. TMDSC experiment were carried out in saw-toothlike modulation with temperature amplitude T_a=0.2 K, modulation period t_p=60 s and a constant underlying cooling rate q_0=0.5 K/min.

4. Results

4.1. Polyvinylacetate PVAC

The DSC thermogram for PVAC was adjusted by six iterations with fixed start values for a series of T_∞ values (Fig. 3). The corresponding sixth fits do not differ by more than 0.01 in dT_f/dT and reproduce the experimental curve reasonably (Fig. 3(A)). The underlying equilibrium trace $\log(2\pi/\tau_b)$ as a function of $1/T_b$ is well defined with a scatter less than a few tenths of a frequency decade for the different T_∞ variants between T=T_g=40.5°C and T=52°C (Fig. 3(B)). This is the informative zone ranging from T_g=40.5°C to T=52°C. It includes the larger part of the step and the overshot of the curve Fig. 3(A). In the informative zone, the $\log(2\pi/\tau_b)$ values from MNM are, within the mutual experimental uncertainty of about 0.3 frequency decades, identical with the frequency $\log \omega_{max}$ values from dielectric $\varepsilon''(\log \omega)$ and HCS $C_p''(\log \omega)$ experiments [34,35]. The experimental uncertainty comes mainly from the mutual uncertainty of temperature definition of the samples in the different apparatuses, ΔT=±1 K. Outside the infor-

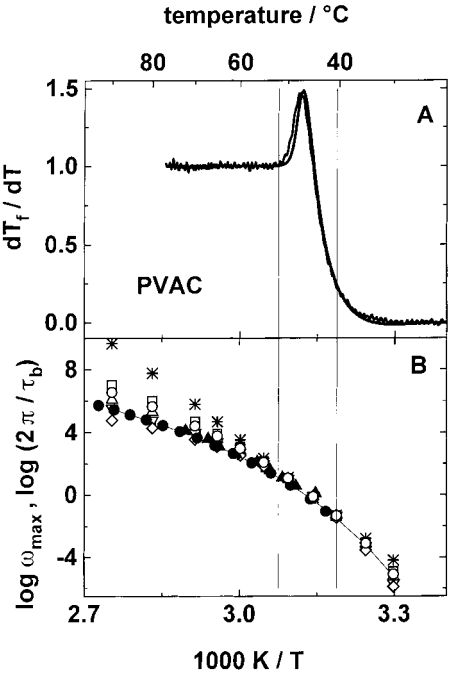

Fig. 3. Dynamic glass transition of PVAC as a function of $1/T$. The informative zone is indicated by the two vertical lines. (A) Reduced heat capacity dT_f/dT (see Eq. (15)) from a DSC heating run after a cooling run, both rates are 10 K/min. (B) Arrhenius diagram with results from different experiments: (●) DK, (▲) HCS, and MNM. For MNM, $\log_{10}(2\pi/\tau_b)$ values were calculated for different T_∞ ((*) T_∞=0 K, (□) −30°C, (○) −20°C, (△) −10°C, (▽) 0°C, (◇) 10°C, (–) fit start values).

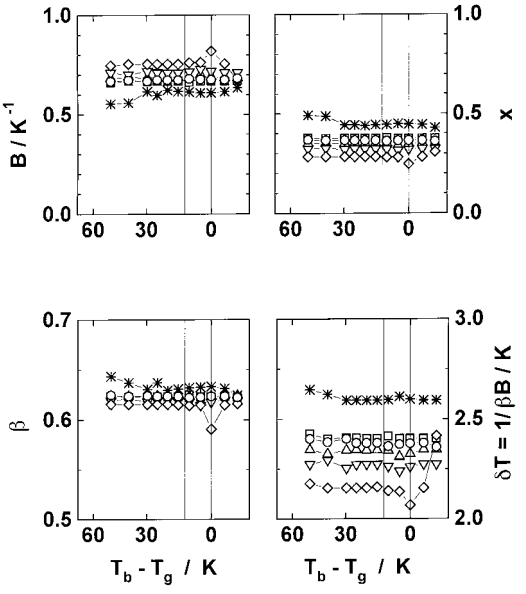

Fig. 4. MNM parameters of sixth fit B, x, β, and δT for PVAC from scanning T_b for different T_∞ ((*) T_∞=0 K, (□) −30°C, (○) −20°C, (△) −10°C, (▽) 0°C, (◇) 10°C). The informative zone is indicated by the two vertical lines.

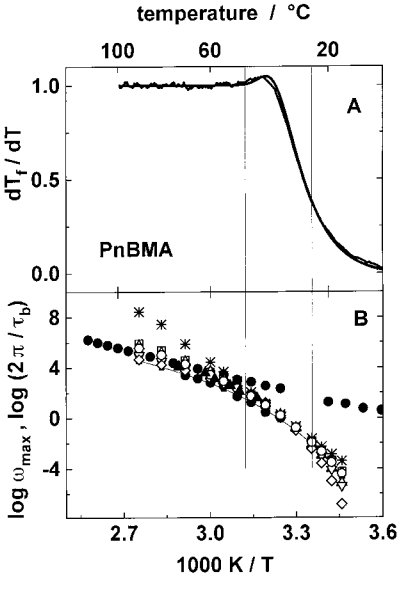

Fig. 5. Dynamic glass transition of P*n*BMA as a function of 1/T. The informative zone is indicated by the two vertical lines. (A) Reduced heat capacity dT_f/dT (see Eq. (15)) from a DSC heating run after a cooling run, both rates are 10 K/min. (B) Arrhenius diagram with results from different experiments: (●) DK, (▲) HCS, and MNM. For MNM, $\log_{10}(2\pi/\tau_b)$ values were calculated for different T_∞ ((*) T_∞=0 K, (□) −45°C, (○) −35°C, (△) −25°C, (▽) −15°C, (◇) −5°C, (–) fit start values).

mative zone the scatter for different T_∞ values is considerable. The best overall coincidence with dielectrics and HCS is obtained for T_∞=0°C, i.e. $T_g - T_\infty$=40 K.

For reasonable T_∞ values the dependence of the B, x, β and δT parameters on the reference temperature T_b is small (Fig. 4). B increases, and x, β, δT decrease with increasing T_∞. The β parameter, characterizing the reciprocal calorimetric width of the α dispersion zone, is little influenced by the T_∞ variations. For T_∞=0°C we obtain in the informative zone for the cooling–heating cycle with $\dot{T}$=10 K/min the following parameters: B=(0.72±0.01)/K, x=0.32±0.01, β=0.62±0.01, δT=(2.2±0.1)K, m_c=98±1.

4.2. Poly(n-butyl methacrylate) PnBMA

The adjustment method was the same as for PVAC. The quality of reproduction of the experimental DSC curve by MNM is comparable with PVAC (Fig. 5(A)). The informative zone is wider than for PVAC. It is ranged from T_g=25°C up to about T=47°C, i.e. its width is 22 K (compared to 12 K for PVAC). This includes about 60% of the ΔC_p step and the weak overshot. The equilibrium trace from MNM is few tenths of a frequency decade above the dielectric trace (see also [28]) and corresponds to the HCS trace in the Arrhenius diagram (Fig. 5(B)).

Outside the informative zone the scatter is again considerable. The $\alpha\beta$ splitting peculiarity is near T=60°C. This is outside the informative zone and can, therefore, not be modeled by MNM. The change of the T_∞=−25°C trace there, from α at low temperatures to a at high temperatures, is considered to be accidental.

The variation of the B, x, β, and δT parameters with T_b is moderate, in particular for reasonably T_∞ values (Fig. 6). The variation of x and B is larger than for PVAC. This indicates the proximity of the crossover. The tendencies with T_∞ are the same as for PVAC. For $T_\infty = T_g - 50$ K=−25°C the following parameters were obtained in the informative zone for the cooling–heating cycle with $\dot{T}$=10 K/min: B=(0.65±0.02)/K, x=0.30±0.01, β=0.31±0.01, δT=(5.0±0.1)K, and

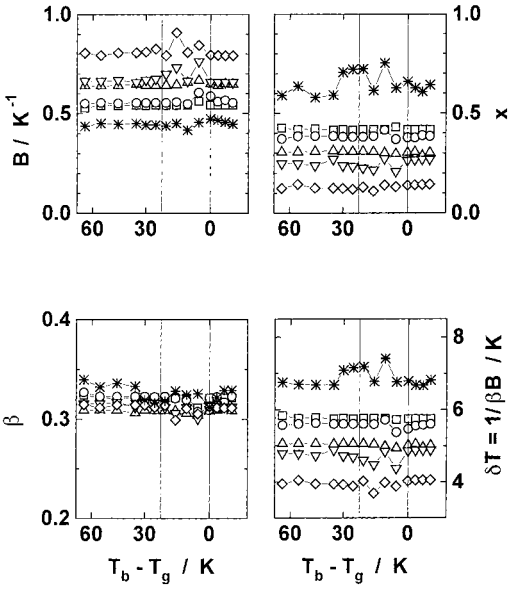

Fig. 6. MNM fit parameters B, x, β, and δT for PnBMA from scanning T_b for different T_∞ ((*) T_∞=0 K, (□) −45°C, (○) −35°C, (△) −25°C, (▽) −15°C, (◇) −5°C)). The informative zone is indicated by the vertical lines.

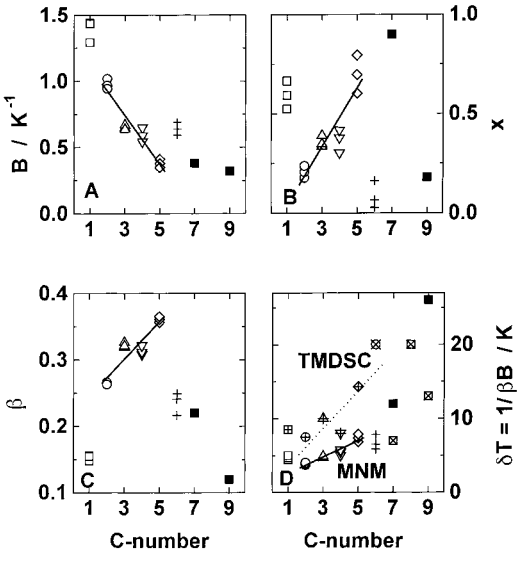

Fig. 7. (A)–(C): MNM fit parameters B, x and β as function of n alkyl side chain length for T_∞=T_g−50 K, T_g−60 K and T_g−70 K. (D) δT was calculated from fit parameters of the average continuation iterations method and from the Gaussian dispersion of TMDSC C_p'' peaks. The linear fits over all values from PEMA to PnPenMA result from DSC (open symbols, solid line) and from TMDSC (crossed symbols, dotted line), respectively. (■) for C=7 and 9 for average continuation iteration method and (☒) for C=7–9 from the Gaussian dispersion of TMDSC C_p'' peaks. (TMDSC: t_p=60 s, temperature amplitude T_a=0.2 K, underlying cooling rate $\dot{T}$ = 0.5 K/min).

m_c=84±2. The small β and the large δT values indicate again the proximity of the crossover.

4.3. Dependence on the C number of the alkyl side group

The parameters B, x, β, and δT for the PnAMA series depend systematically on the C number from C=2 (ethyl) to C=5 (pentyl). In Fig. 7, the parameters are calculated with fixed start values for three T_∞ variants: T_g−50 K, T_g−60 K, and T_g−70 K. The variations with T_∞ do not destroy the trends in this C number range: B decreases (this corresponds to decreasing fragility), x increases dramatically, β increases, and δT increases with increasing C number. This corresponds to approaching the crossover region from the α side. The methyl member (PMMA) is outside the trend. The tacticity of our PMMA sample is different from the others. Furthermore, peculiarities are often observed for the methyl member of homologous series. The δT parameter is larger for TMDSC with a time period of t_p=60 s. This corresponds to a general trend for the α transition [35]: δT increases along the α-trace with increasing frequencies and temperature [34,36], i.e. with decreasing time periods (T_g corresponds to a larger period of order t_p=1000 s).

The hexyl member (PnHMA) does not fit to the C=2, . . . , C=5 trend. We arrived at the crossover region. The DSC and TMDSC scans for the pentyl and hexyl member are compared in Fig. 8. The dramatic x change between C=5 and C=6 cannot explicitly be seen in the thermograms. The compensation possibilities in the four-dimensional Narayanaswamy parameter space are large [37]. To prove what happens beyond C=6 the parameters for C=7 and C=9 are added (Fig. 7). All parameters for C=7 and C=9 are calculated by six average continuation iterations for T_∞=T_g−50 K. The β-value for C=9 is unexpectedly small (β=0.12). An influence of the α_{PE} glass transition cannot completely be excluded. For the C=2, . . . , C=5 range the trends of Fig. 6 are exactly reproduced. For C=9 we are above the crossover region, i.e. in the high-temperature a relaxation. The decrease of fragi-

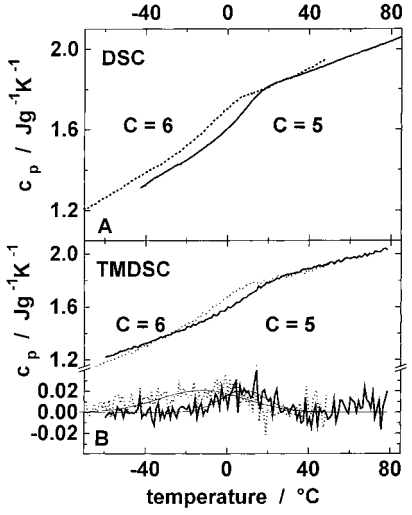

Fig. 8. (A) C_p from DSC heating run with $\dot{T} = 10$ K/min. (B) Real and imaginary parts of C_p^* from TMDSC (t_p=60 s, temperature amplitude T_a=0.2 K, underlying cooling rate $\dot{T} = 0.5$ K/min) for P*n*Pe*n*MA (solid line) and P*n*HMA (dotted line).

lity (B) continues, the width of the a dispersion zone increases (β decreases), the mixing parameter x remains small, but δT behaves irregularly.

Unfortunately, the scenario for C>6 becomes more complicated than expected from Fig. 1. Besides the a relaxation, a new relaxation with increasing T_g and increasing intensity enters [32]. This is the α_{PE} transition introduced by Heijboer [30,31].

Recently, a complementary investigation on poly(methyl α-alkyl acrylate)s were presented, i.e. investigations on the enlargement of the α-methyl group [38]. The parameter x increases and Δh decreases with increasing C number of the side chain, whereas β remains constant. A drastic change of the behavior appears at about C=5. The results are explained [38] on the basis of modifications of the interchain interactions: increasing α-side chains lead to an increase of the distance between the main chains and a decrease of the interchain interactions.

5. Discussion

5.1. Narayanaswamy parameters for PVAC and PS

Our procedure for PVAC was also applied to polystyrene PS. The tendencies are the same as for PVAC (Table 2). The parameters for T_∞=0 are quite different from the literature values compiled by Hodge [29], especially for x. For PVAC, our x is significantly larger (x_{MNM}=0.45±0.01, x_H=0.27, ..., 0.41), and for PS, our x is significantly smaller (x_{MNM}=0.39, x_H=0.44, ..., 0.52) than the Hodge values. The discrepancies are damped for PVAC and sharpened for PS when reasonable T_∞ values are formally included in the comparison.

The reasons for the discrepancies are not clear as yet. One possibility would be a large sensitivity to molecular details (such as molecular weight distribution, tacticity, branching etc.). This would deserve systematic investigations. A second possibility would be that the $T(t)$ programs used for DSC are not exactly the same. Another possibility would be hidden differences in the adjustment procedures. Until clarification, the Narayanaswamy mixing parameter x should be interpreted with caution: only dramatic tendencies or discrepancies can reasonably be interpreted by physical arguments concerning the glass transition phenomenon directly.

5.2. Derived parameters along the homologous series

The tendencies for the C=2, ..., C=5 range obtained from the iterations with fixed start values are collected in Fig. 9. The square root of cooperativity, $N_\alpha^{1/2}$, tends linearly to $N_\alpha^{1/2} = 1$ that would be arrived for the hexyl member (Fig. 9(A)). This tendency is the typical behavior for the α relaxation below the crossover [7,23,34]. This behavior is not destroyed by the T_∞ variations. The same dependence is obtained from TMDSC at t_p=60 s time period. The $N_\alpha^{1/2}$ values from TMDSC are smaller, corresponding to the smaller distance from the onset in the crossover region. The corresponding characteristic lengths ξ_α decrease from about 2 nm for the ethyl member to about 1 nm for the pentyl member (Fig. 9(B)). This length is defined by $V_\alpha = \xi_\alpha^3$, where V_α is the volume of N_α monomeric units. The glass temperatures for $\dot{T}$=10 K/min and for t_p=60 s decrease linearly with the C number (Fig. 9(C)). The relation [34] between cooling rate, $\dot{T}$, reduced by δT, and glass frequency, $\omega_{max}=2\pi/\tau_b$ at T_g, shows no clear tendency (Fig. 9(D)). The theoretical value for the "vitrification rate" $a = \dot{T}/\omega_{max}\delta T$ [21,22] is a=5.5±0.1, corre-

Table 2
Narayanaswamy parameters from literature [29] and from MNM for PVAC and PS

		T_g (K)	T_∞ (K)	$\Delta h'/R$ (kK)	x	β	$-\ln A^a$ (s)
PVAC	Sasabe	310	0	71	0.41	0.51	223.6 [46]
	Hodge		0	71	0.41	0.51	223.6 [47]
	Hodge		0	88	0.27	0.51	277.5 [48]
	MNM	313.5	0	60	0.45	0.63	182.9
			243	66	0.37	0.62	42.1
			253	67	0.36	0.62	35.8
			263	68	0.35	0.62	29.7
			273	72	0.32	0.62	23.9
			283	78	0.25	0.59	19
PS	Hodge	373	0	80	0.46	0.71	216.0 [48,49]
	Hutchinson	373	0	70	0.46	–	– [50]
	Prest	373	0	53–71	0.52	0.8	– [51]
	Privalko	373	0	76–110	0.44	0.55	– [52]
	Oudhuis	373	0	126	0.24	0.47	329 [53]
	MNM	373	0	92	0.39	0.58	231
			303	104	0.30	0.57	51
			313	103	0.30	0.57	40
			323	107	0.27	0.56	33.5
			333	110	0.24	0.56	26.1
			343	119	0.20	0.55	17.1

[a] A is the time prefactor of the Vogel Tamman Fulcher (VTF) equation, $\tau = A \exp(B/T - T_\infty)$. For $\log \Omega = \log(2\pi/\tau) = 12$ in Eq. (7) it follows $-\ln A = 25.8$, τ in seconds. $|\ln A| > 30$ values are not reasonable.

sponding to $\log a = 0.74$. The maximal deviation is observed for the pentyl member: the observed value is only 10% of the theoretical value. The vitrification of complicated $C''_p(\log \omega)$ spectra [28] in the crossover region does not correspond to the simple situation supposed for the theoretical value [39].

In the crossover region, C=5, ..., C=7, we have certainly $C''_p(\log \omega)$ spectra that are not consistent with a Kohlrausch function Eq. (9)[39] as used in our MNM. All MNM parameters for this C range must therefore be handled with caution.

The full range (C=1, ..., C=9) tendencies as obtained from the average continuation iterations are collected in Fig. 10. The crossover between α and a relaxations near C=6 is indicated by a sharp bend in the $N_\alpha^{1/2}$ plot (Fig. 10(A)). The cooperativity of the a process remains small, $N_\alpha^{1/2}$ is of order 1 there. A dramatic, jump-like decrease of the Narayanaswamy mixing x parameter at the crossover can clearly be seen in the x versus T_g diagram (Fig. 10(B)). The x parameter remains small ($x<0.25$) for the high-temperature a process.

In a speculation, the small x parameters for the a process can be connected with small $N_\alpha \approx 1$ values. Approaching the crossover from the α side, the cooperativity N_α decreases and x increases. The latter means that the vitrification during linear cooling is increasingly determined by the actual temperature, i.e. decreasingly determined by the fictive temperature, see Eq. (14). The fictive temperature indicates the effect of preceding freezing-in [40]. Increasing x means, therefore, that the effect of preceding freezing-in decreases. Having a certain cooperativity, as for α, the freezing first affects the cooperative environment of the Glarum defect diffusion [41,42]. Decreasing N_α means to have lesser cooperativity whose freezing can affect the relaxation: x must increase. But the situation is changed above the crossover, i.e.

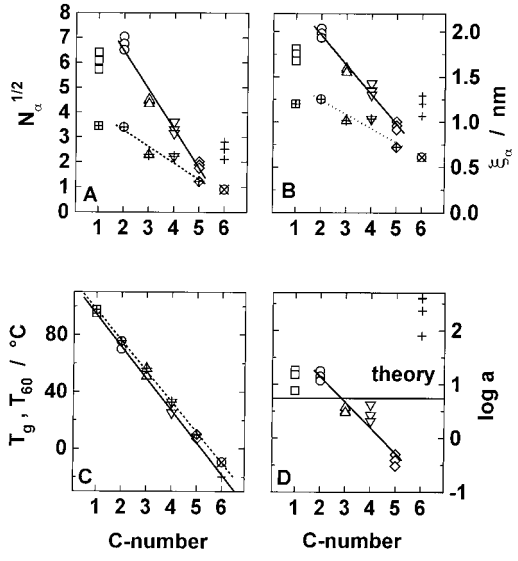

Fig. 9. Square root of cooperativity $N_\alpha^{1/2}$ (A) and characteristic length ξ_α (B) calculated from MNM fit parameters (fits with T_∞=T_g−50 K, T_g−60 K, and T_g−70 K) (open symbols) and from TMDSC (t_p=60 s, temperature amplitude T_a=0.2 K, underlying cooling rate $\dot{T}$ = 0.5 K/min) (crossed symbols). (C) T_g from DSC (10 K/min) and T_{60} (t_p=60 s) from TMDSC. (D) α process vitrification rate a=$T/\delta T\omega$ with ω =$2\pi/\tau_b$ for T_b=T_g.

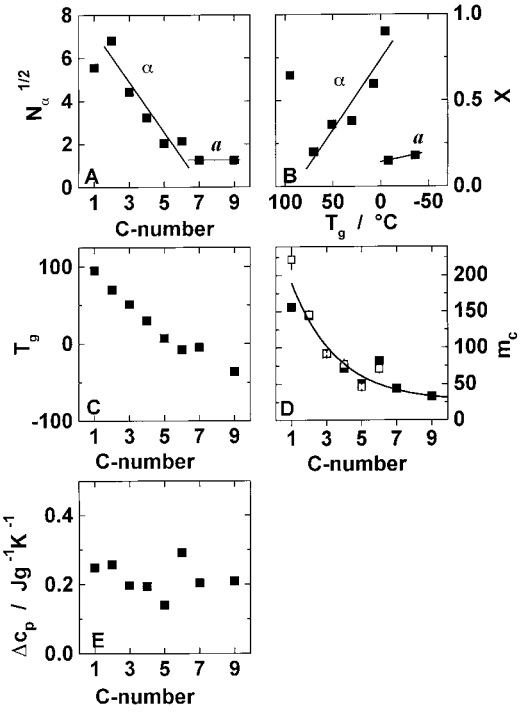

Fig. 10. $N_\alpha^{1/2}$ (A), x (B), T_g (C), fragility m_c (D), (■) "average continuation iteration" and (□) "fixed start values" methods) and ΔC_p (E) for C numbers 1–9 of the alkyl side chain. All points are MNM sixth fit results for T_∞=T_g−60 K for "average continuation iterations".

for the a process. N_α≈1 indicates that there is no cooperativity at all. The only process is diffusion by cage escape [28]. Freezing affects the cage directly, i.e. the relaxation is fully determined by the fictive temperature: x remains small, therefore.

The T_g versus C number diagram shows a small irregularity at C=6 and C=7 (Fig. 10(C)). The x versus C number diagram reflects this irregularity, in contrast to the regular x versus T_g diagram (Fig. 10(B)).

The fragility steepness index m_c dramatically decreases with the alkyl side-group length (Fig. 10(D)). After a certain irregularity at the cross-over (C=6), the m_c values further decrease for the a process, down to small m_c=33 values. The fragility for the a process is smaller than for the α process. This corresponds to small or missing cooperativities with correspondingly low [25] Vogel temperatures T_∞ [43–45].

The ΔC_p steps do not show a clear tendency for C≥6 (Fig. 10(E)). This may be caused by a second glass transition in the P*n*AMA series, assigned to a supposed polyethylene-rich nanophase [32] in the P*n*AMAs for higher C numbers. The corresponding T_g and its intensity ΔC_p increase with the C number. This enlarges the uncertainty of any tangent construction to determine ΔC_p for the a process.

The MNM equilibrium traces for T_∞=T_g−60 K and the TMDSC glass temperatures for τ_p=60 s are compared with the dielectric traces for C=1, . . ., C=6 in an Arrhenius diagram (Fig. 11). For low frequencies all three methods are consistent to a reasonable degree. The decrease of fragility with increasing C number is indicated by the decreasing slopes of the MNM points from DSC. At high frequencies, the MNM frequencies for PMMA and PEMA are much larger than the dielectric frequencies. This demonstrates the units of MNM and is caused by the average continuation iteration as used far above the informative zone. Such an iteration cannot find the secondary optimization minimum of the a process.

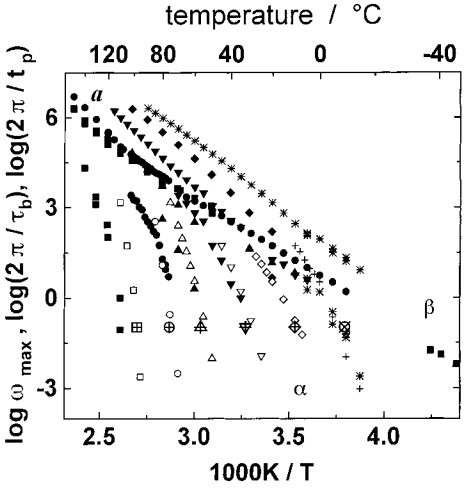

Fig. 11. Arrhenius plot for poly(*n*-alkyl methacrylate)s (PMMA (■), PEMA (●), P*n*PrMA (▲), P*n*BMA (▼), P*n*PenMA (◆), P*n*HMA (*)) from DK (solid symbols), TMDSC for t_p=60 s (big crossed symbols, P*n*HMA (⊗)), and DSC $\log(2\pi/\tau_b)$ with τ_b (s) for fits with $T_\infty = T_g - 60$ K (open symbols, P*n*HMA (+)). For DSC, only the results in the informative zone are indicated.

6. Conclusions

In the frequency–temperature domain, for a given substance, the crossover region of dynamic glass transition separates a high-temperature *a* process from the cooperative low-temperature α process. In the homologous series of poly(*n*-alkyl methacrylate)s P*n*AMAs, i.e. in the C number domain for a given DSC cooling rate $\dot{T}$ or TMDSC frequency, the crossover region separates the *a* process at high C numbers from the cooperative α process at low C numbers. The crossover for $\dot{T} = 10\,\mathrm{K/min}$ is marked by C=6, i.e. by poly(*n*-hexyl methacrylate), P*n*HMA.

A test with the modified Narayanaswamy model MNM for ordinary polymers as PVAC and PS indicates that at present the Narayanaswamy mixing parameter x has no definite meaning related to the substance as such, e.g. PVAC or PS. Instead it depends on unknown details of the substance or the temperature–time program or the evaluation method. The uncertainty is perhaps $\Delta x = \pm 0.2$ for moderate changes of the unknown.

The increase of x along the α process in the homologous P*n*AMA series is dramatic, however, practically from zero to one from ethyl to pentyl, so that an interpretation seems meaningful. Moreover, for the *a* process, the x parameter remains small, $x<0.25$. We assume that such strong x trends, clearly beyond the uncertainty mentioned above, can be interpreted in terms of the two processes separated by the crossover. The different x behavior in α and *a* is explained by a speculation about different cooperativities: for the *a* process we need no intermolecular cooperativity so that small x values correspond to a sudden vitrification of the cage escape process, assumed to be typical for the *a* process. For the α process we use the hypothesis that cooperativity is a property of the cage environment, a cooperativity shell around the Glarum defect, assisting the escape. The large x at small (but different from zero) cooperativity, as for the pentyl member, corresponds to a sudden freezing of the cooperativity shell with only a small effect on escaping: $x \approx 1$ corresponds to the control by only the actual temperature. For increasing cooperativities (as for decreasing C number: C=4, C=3, etc.) the effect of preceding freezing on the relaxation increases, which means decreasing x.

Acknowledgements

We thank Drs. M. Beiner and K. Schröter for a detailed discussion of the α_{PE} glass transition in higher P*n*AMAs, especially for using their unpublished experimental results for our discussion, Dr. S. Zeeb for the synthesis of higher P*n*AMAs (P*n*PrMA, P*n*PenMA, P*n*HepMA, P*n*LMA), and Dr. G. Meier for providing the P*n*HMA sample. We thank the Deutsche Forschungsgemeinschaft DFG (Sonderforschungsbereich 418) and the Fonds Chemische Industrie FCI for financial support.

References

[1] J.L.G. Ribelles, M.M. Pradas, A.V. Garayo, F.R. Colomer, J.M. Estellés, J.M.M. Dueñas, Macromolecules 28 (1995) 5878.
[2] V.A. Bershtein, V.M. Egorov, Differential Scanning Calorimetry of Polymers, Ellis Horwood, New York, 1994.
[3] E. Hempel, M. Beiner, T. Renner, E. Donth, Acta Polym. 47 (1996) 525.
[4] J.M.G. Cowie, S.A.E. Henshall, I.J. McEwen, J. Velikovic, Polymer 18 (1977) 612.

[5] E. Flikkema, G.A. van Ekenstein, G. ten Brinke, Macromolecules 31 (1998) 892.
[6] M. Beiner, J. Korus, E. Donth, Macromolecules 30 (1997) 8420.
[7] M. Beiner, S. Kahle, E. Hempel, K. Schröter, E. Donth, Europhys. Lett. 44 (1998) 321.
[8] Y. Ishida, K. Yamafuji, Kolloid Z. 177 (1961) 98.
[9] N.G. McCrum, B.E. Read, G. Williams, Anelastic and Dielectric Effects in Polymer Solids, Wiley, London, 1967.
[10] F. Garwe, A. Schönhals, H. Lockwenz, M. Beiner, K. Schröter, E. Donth, Macromolecules 29 (1996) 247.
[11] W. Götze, in: J.P. Hansen, D. Levesque, J. Zinn-Justin (Eds.), Liquids, Freezing and the Glass Transition, Proceedings of Les Houches Summer School, North-Holland, Amsterdam, 1989, p. 1.
[12] J. Heijboer, in: J.A. Prins (Ed.), Physics of non-crystalline solids, Proceedings of the International Conference, Delft, July 1964, North-Holland, Amsterdam, 1965, p. 231.
[13] S.C. Kuebler, D.J. Schaefer, C. Boeffel, U. Pawelzik, H.W. Spiess, Macromolecules 30 (1997) 6597.
[14] K. Kishimoto, H. Suga, S. Seki, Bull. Chem. Soc. Jpn. 46 (1973) 3020.
[15] O.S. Narayanaswamy, J. Am. Ceram. Soc. 54 (1971) 491.
[16] A.Q. Tool, J. Am. Ceram. Soc. 29 (1946) 240.
[17] C.T. Moynihan, A.J. Easteal, M.A. DeBolt, J. Am. Ceram. Soc. 59 (1976) 12.
[18] G. Williams, D.C. Watts, Trans. Faraday Soc. 60 (1970) 80.
[19] D.J. Plazek, K.L. Ngai, Macromolecules 24 (1991) 1222.
[20] M.L. Williams, R.F. Landel, J.D. Ferry, J. Am. Chem. Soc. 77 (1955) 3701.
[21] E. Donth, S. Kahle, J. Korus, M. Beiner, J. Phys. I France 7 (1997) 581.
[22] J. Korus, E. Hempel, M. Beiner, S. Kahle, E. Donth, Acta Polym. 48 (1997) 369.
[23] S. Kahle, J. Korus, E. Hempel, R. Unger, S. Höring, Macromolecules 30 (1997) 7214.
[24] E. Donth, J. Noncryst. Solids 53 (1982) 325.
[25] E. Donth, Relaxation and Thermodynamics in Polymers. Glass Transition, Akademie-Verlag, Berlin, 1992.
[26] E. Donth, J. Polym. Sci. B 34 (1996) 2881.
[27] A. Brunacci, J.M.G. Cowie, R. Ferguson, J.L.G. Ribelles, A.V. Garayo, Macromolecules 29 (1996) 7976.
[28] S. Kahle, E. Hempel, M. Beiner, R. Unger, K. Schröter, E. Donth, J. Mol. Struct., in press.
[29] I.M. Hodge, J. Noncryst. Solids 169 (1994) 211.
[30] J. Heijboer, Stat. Dyn. Prop. Polym. Solid State 94 (1982) 197.
[31] J. Heijboer, M. Pineri, in: G. Harting, D. Evans (Eds.), Nonmetallic Materials and Composites at Low Temperatures, vol. 2, Plenum Press, New York, 1982, p. 89.
[32] M. Beiner, K. Schröter, E. Hempel, S. Reissig, E. Donth, Macromolecules 31 (1998) 8973.
[33] E. Donth, Relaxation and Thermodynamics in Polymers. Glass Transition, Chapter 7, Akademie-Verlag, Berlin, 1992.
[34] E. Donth, J. Korus, E. Hempel, M. Beiner, Thermochim. Acta 304/305 (1997) 239.
[35] J. Korus, Wärmekapazitätsspektroskopie (3ω-Methode) an Polymeren: Temperaturabhängigkeit der Kooperativität des dynamischen Glasübergangs, Thesis, Universität Halle, 1997.
[36] S. Weyer, A. Hensel, J. Korus, E. Donth, C. Schick, Thermochim. Acta 304/305 (1997) 251.
[37] C. Schneider, Die gegenseitige Anordnung unterschiedlicher Signale des Glasübergangs amorpher Polymere, Thesis, Merseburg, 1984.
[38] M.-E. Godard, J.-M. Saiter, P. Cortés, S. Montserrat, J.M. Hutchinson, F. Burel, C. Bunel, J. Polym Sci. B 36 (1998) 583.
[39] E. Donth, to be published.
[40] F. Simon, Ergeb. exakt. Naturwiss. 9 (1930) 222.
[41] S.H. Glarum, J. Chem. Phys. 33 (1960) 639.
[42] G. Adam, J.H. Gibbs, J. Chem. Phys. 43 (1965) 139.
[43] J.-F. Stickel, Untersuchungen der Dynamik in niedermolekularen Flüssigkeiten mit Dielektrischer Spektroskopie, Thesis, Mainz 1995, Shaker, Aachen, 1995.
[44] F. Stickel, E.W. Fischer, R. Richert, J. Chem. Phys. 102 (1995) 6251.
[45] F. Stickel, E.W. Fischer, R. Richert, J. Chem. Phys. 104 (1996) 2043.
[46] H. Sasabe, C.T. Moynihan, J. Polym. Sci. 16 (1978) 1447.
[47] I.M. Hodge, J. Noncryst. Solids 131–133 (1991) 435.
[48] I.M. Hodge, Macromolecules 20 (1987) 2897.
[49] I.M. Hodge, Macromolecules 16 (1983) 898.
[50] J.M. Hutchinson, M. Ruddy, Polym J. Sci. B 26 (1988) 2341.
[51] W.M. Prest Jr., F.J. Roberts, I.M. Hodge, in: J.C. Buck (Ed.), Proceedings of the Twelfth NATAS Conference, NATAS, 1983.
[52] V.P. Privalko, S.S. Demchenko, Yu.S. Lipatov, Macromolecules 19 (1991) 121.
[53] A.A.C.M. Oudhuis, G. ten Brinke, Macromolecules 25 (1992) 698.